

PERFORMANCE COMPARISON OF TWO MEDIUM TEMPERATURE PACKED BED LATENT HEAT STORAGE SYSTEMS DURING CHARGING

Ashmore Mawire¹, Chidiebere Ekwomadu¹, Tlotlo Lefenya¹ and Adedamola Shobo²

¹ North-West University, Department of Physics and Electronics, Private Bag X2016, Mmabatho 2745, South Africa

² Department of Mathematics, Science and Sports Education, University of Namibia, Private Bag 5507, Oshakati, Namibia

Abstract

Two packed bed latent heat storage systems for medium temperatures are experimentally compared during charging cycles. The first storage system consists of a packed bed of spherically encapsulated eutectic solder (Sn67Pb37). The second latent heat storage is a cascaded system consisting of 20 spherically encapsulated eutectic solder capsules at the top of the storage and 20 spherically encapsulated erythritol capsules at the bottom in a storage ratio of 1:1. Sunflower Oil is used as the heat transfer fluid for the experiment tests. The cascaded latent heat shows greater values of the charging energy and exergy rate since two phase change transitions for the eutectic solder and erythritol release greater latent heat than the single PCM system during low flow-rate charging (4 ml/s). For charging with a high flow-rate (8 ml/s), the cascaded storage system shows better energy and exergy charging rates before the bottom PCM melts. After melting of the lower temperature PCM at the bottom, the temperature increases at the bottom of the cascaded system and the single PCM system shows higher charging energy and exergy rates.

Keywords: Charging; Cascaded latent heat storage; Erythritol; Eutectic solder; Packed bed latent heat storage

1. Introduction

Latent heat storage systems have the advantages of a higher thermal energy storage density and a nearly isothermal behaviour during the storage and release of energy as compared to sensible heat storage systems. There have been limited recent studies on packed bed latent heat storage using oil packed bed TES systems for medium to high temperature applications [1-2]. Using oil instead of air is justified by the fact that a lower pumping power is required and the design of the storage system is less complicated since fewer pressurized components are required. Sunflower Oil has been selected as a heat transfer fluid (HTF) since it is cheap, food grade and readily available, non-toxic and possesses characteristics comparable to other commercial HTFs as previously investigated in [3]. Erythritol has recently been proposed as a suitable phase change material (PCM) for medium temperature applications [4], but no study has ever been done on it in a packed bed cascaded storage configuration. Limited recent work has also suggested metallic solders [5-6] as suitable PCMs for medium temperature domestic applications to cater for drawbacks of super-cooling exhibited by organic and inorganic PCMs.

Cascaded thermal energy storage (TES) systems using two or more phase change materials (PCMs) are a recent innovation and experimental literature is limited to only a few recent papers [7-8], especially for medium to high temperatures. The results of the cascaded systems [7-8] showed better performance as compared to single PCM based systems. The aim of the paper is thus to compare a single PCM eutectic solder packed bed latent heat TES system with a two PCM (eutectic solder/erythritol) packed bed cascaded system during charging cycles using Sunflower Oil as the heat transfer fluid. The work presented will add to the limited experimental work that has been done on metallic PCM systems and cascaded TES systems. To the best of our knowledge, no cascaded system using a metallic PCM and an oil HTF has ever been reported.

2. Experimental setup and procedure

Erythritol was poured into twenty spherical aluminum capsules with diameters of 0.05 m and wall thicknesses of 0.001 m. The capsules were manufactured as hollow spheres with openings at the top to allow for pouring of PCM. The volume of the PCM in the capsules was about 80 % of the total internal volume of the capsule to allow for thermal expansion. The volume to be poured into the capsule was measured very carefully with a small measuring cylinder. Small crystals of erythritol were used so that it could be poured easily in its solid form into the capsules. After pouring of erythritol, two capsules of erythritol had K-thermocouples fixed onto them to measure the PCM temperatures. These thermocouples which extended into the centre of the spheres were fastened on the top of the spheres. The thermocouples acted both as sealing mechanisms and also as temperature monitoring devices. The rest of the PCM capsules were sealed with screw caps. Fig. 1 shows a PCM capsule with a screw cap and one with a thermocouple screw cap. Extra care was taken to ensure that approximately the same mass of erythritol was placed inside each capsule. The total mass of each capsule was measured before and after encapsulation with an electronic balance to ensure that the capsules had almost the same mass of PCM inside them. Erythritol capsules were heated up to their melting points in an oil bath to ensure that there were no PCM leakages before they were put into the storage tank.

The process for encapsulating the eutectic solder was slightly different. 2 mm thick solder wire was inserted into each of the 40 capsules from the top opening until a volume an internal volume 80 % was covered. A screw driver was used to press down on the solder wire to ensure that the solder occupied the maximum volume. Care was taken to ensure that all 40 capsules had approximately the same mass of solder inside them as with case of erythritol. The melting procedure was done with the eutectic solder capsules to check for PCM leakages before inserting them into the storage tank.

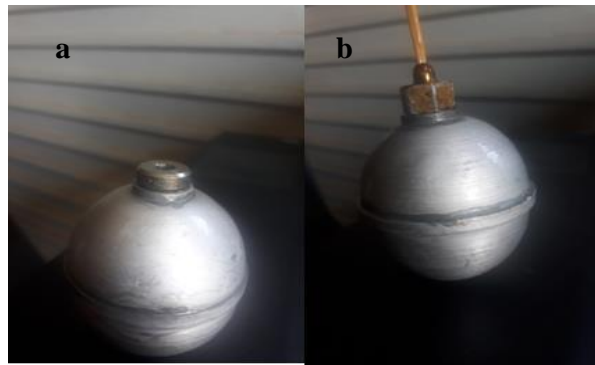


Figure 1. (a) Aluminium PCM capsule with screw cap. (b) Aluminium capsule with thermocouple screw cap [5].

Thermo-physical properties of erythritol and the eutectic solder obtained from open literature are shown in Table 1. The mass of erythritol inside each capsule was around 44 g. The mass of the eutectic solder inside each capsule was around 164 g because of its higher density. The thermal conductivity of the solder is higher than for erythritol. Due to the expensive nature of the equipment involved in measuring thermal properties quoted experimental values obtained from literature are used. Besides, previous work has been done on the thermal properties and the scope of this study is limited to the bulk performance of PCM capsules in a storage tank which make up the single PCM and the cascaded PCM storage system. No work has been previously reported on the bulk performance of these systems in a packed bed storage configuration.

Table1. Thermo-physical properties of the two PCMs

Property	Erythritol	Eutectic (Sn63/Pb37) Solder
Melting Temperature (°C)	118-122 [5]	183 [9, 11]
Specific Heat Capacity (kJ/kgK)	1.38 (20 °C), 2.76 (140°C) [5]	0.21 (30 °C) ([9]
Phase change enthalpy (kJ/kg)	139.7 [5]	52.1 [10]
Density(kg/m ³)	1210 [5]	8400 [11]
Thermal conductivity (W/mK)	0.130 (120 °C) [5]	50 [11]
Average mass of PCM in the capsule (g)	44	164

The experimental schematic of the TES system is shown in Fig. 2. The first storage system was filled with 40 eutectic solder (Sn67Pb63) PCM capsules up to Level A. For the second cascaded storage system, the top half of the storage tank was filled eutectic solder spherical capsules (20), while the bottom half was filled with erythritol capsules (20) in a 1:1 storage ratio. The void between the capsules/ was filled with Sunflower Oil up to level A.

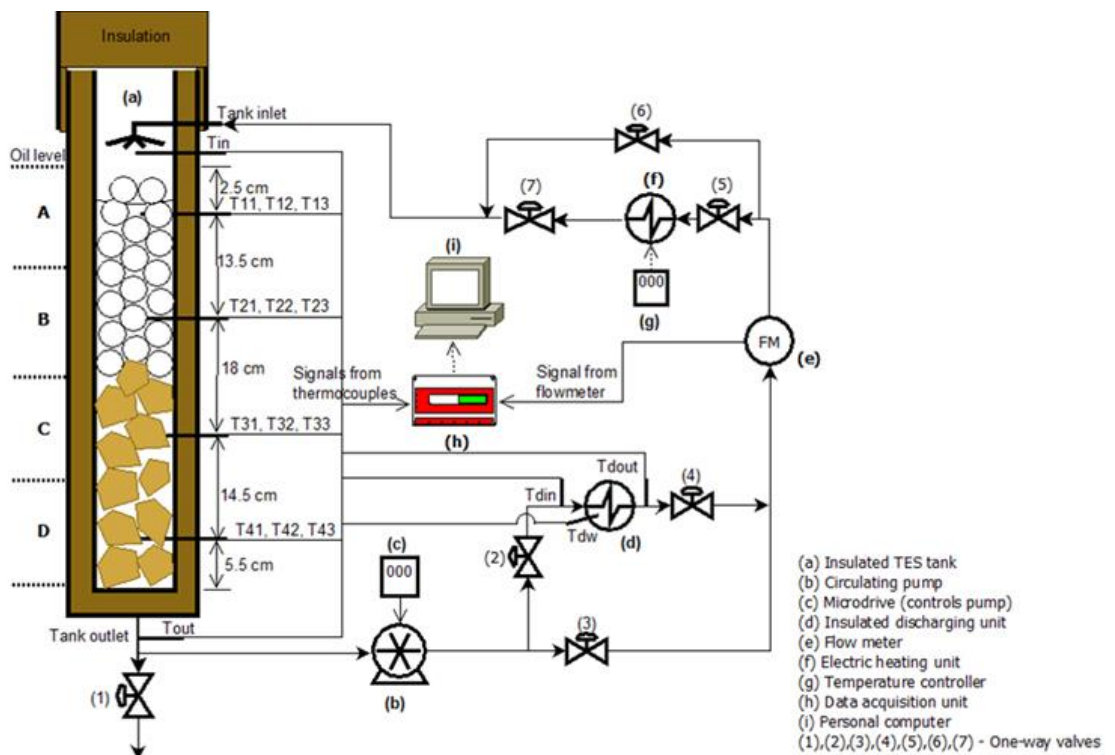


Figure 2. Schematic diagram of experimental setup [12, 13].

The electric unit (f) consisted of two copper spiral coils (power rating: 220V, 900 W each) to heat up the

circulating oil and it was controlled by a temperature controller. The TZN4S temperature controller (g) (display accuracy: ± 0.3 %) was used to set and control the required maximum temperature. An insulated stainless steel cylindrical storage tank (a) with a diameter of 0.3 m and a height of 0.54 m was used. K-type thermocouples (accuracy: ± 1 %) were placed at radial distances of 0.013 m, 0.038 m and 0.064 m to measure temperature at each axial level of the storage tank (Levels A-D). During the charging cycles valves (1), (2), (4) and (6) were closed while valves (3), (5), (7) were opened.

3. Experimental thermal analysis

The charging energy rate (power) depends on the inlet and outlet charging temperatures of the storage tank and is expressed as

$$\dot{E}_{ch} = \rho_{av} c_{av} \dot{v}_{ch} (T_{chin} - T_{chout}) \quad (1)$$

, where ρ_{av} is the temperature dependent average density of the oil, c_{av} is the temperature dependent average density of the oil, \dot{v}_{ch} is the volumetric charging flow-rate, T_{chin} is the inlet charging temperature at the top of the storage tank and T_{chout} is the outlet charging temperature at the bottom of the storage tank. The charging exergy rate is given as;

$$\dot{E}_{xch} = \rho_{av} c_{av} \dot{v}_{ch} \left[(T_{chin} - T_{chout}) - \left(T_{amb} \ln \frac{T_{chin}}{T_{chout}} \right) \right] \quad (2)$$

, where T_{amb} is the ambient temperature.

4. Results and discussion

Storage tank profiles for the two systems for low (4 ml/s) and high charging flow-rates (8 ml/s) are shown in Fig. 3. The charging times for the two storage systems are seen to increase with an increase in the flow-rate. The increase in the charging time with flow-rate has also been reported in previous work done using the same storage system [12-13]. This is because of the increased cooling effect induced by the higher flow-rate on the electrical heater which tends to lower the inlet charging temperature for the higher flow-rate such that the bottom experimental limiting charging temperatures are approached at later times. Charging of the single PCM system is terminated when the bottom temperature of the storage (T_D) is around 190 °C to ensure melting of the PCM at the bottom for the single PCM base system. Eutectic solder has a melting temperature of around 183 °C, and this temperature ensured melting at the bottom. For the cascaded storage system, charging is terminated when the temperatures of the bottom storage temperature (T_D) are around 180 °C to ensure that the flash point temperature of erythritol is not exceeded. The flash point temperature of erythritol is around 190 °C, and as a safety precaution the lower bottom temperature of the cascaded system is limited to 180 °C.

The phase change process is seen to progress from the top to the bottom of the storage tank for the single PCM system. The phase change process at the top of the storage tank (T_A) starts at around 90 mins with the lowest flow-rate since charging is from the top to the bottom of the storage tank. On the other hand, due to the lower melting point PCM at the bottom of the storage tank, the phase change process for the cascaded system starts at around 50 mins with T_C showing the first phase change transition, followed by T_D . The top storage tank temperatures only show phase change transitions after 100 mins for the cascaded system. It is also important to note that with an increase in the charging flow-rate, the phase change processes commence at later times for both storage systems. The increase in the flow-rate increases the heat transfer rates. This causes the rate of temperature rise in the storage tank to be faster thus lowering the axial thermal gradients and the degree of thermal stratification. The bottom limiting storage tank temperatures are also approached at later times which effectively increases the charging times for both storage systems.

The axial thermal gradients for the cascaded storage system during the charging cycles are more pronounced for the cascaded system implying more axial thermal stratification for the cascaded system. It is also important to note that the outlet charging temperature is affected by the phase change process and it shows a similar variation to the bottom storage tank temperature, T_D . For the cascaded system, the phase change transition of erythritol is well depicted by the variation of the outlet charging temperature. For the single PCM system, the variation of the outlet temperature during the phase change process at the bottom of the storage tank is not as pronounced as compared to the cascaded system. The outlet charging temperature also increases with an increase in the flow-rate. Slightly higher TES temperatures are seen with the single PCM system at the end of charging as compared to the cascaded system possibly due to the higher charging termination temperatures at the bottom of the storage tank.

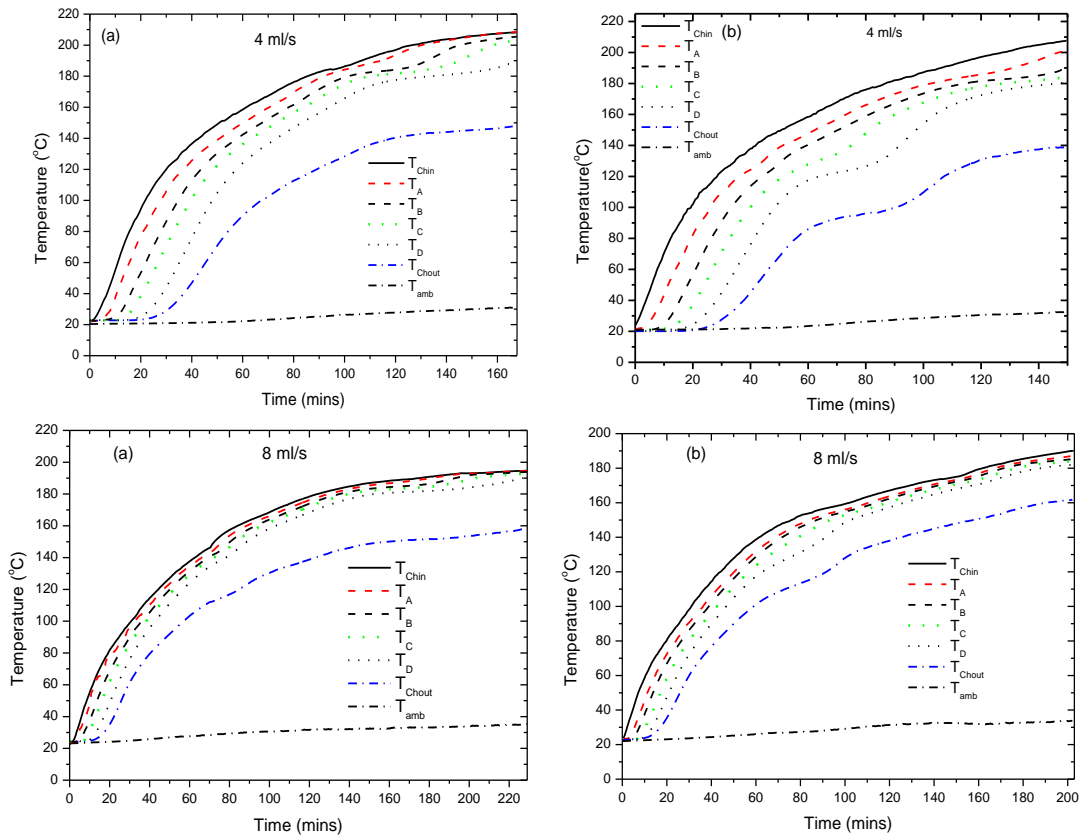


Figure 3. Storage tank charging profiles for (a) the single PCM and (b) the cascaded two PCM system for low (4 ml/s) and high (8 ml/s) flow-rates.

To evaluate the quantity of the stored energy and the rate at which it is stored during the charging cycles, charging energy rate profiles are presented in Fig. 4. For the lowest flow-rate, the single PCM eutectic solder TES shows generally higher values of the energy rate for the whole duration of charging. The charging energy rates for the two storage systems initially rise quickly to peak values during the initial stages of charging since the bottom outlet temperatures are low causing large initial axial thermal gradients which induce the rapid rise to the peak values. As the bottom outlet temperatures progressively rise, the charging energy rates drop from the peak values. For the lowest charging flow-rate (4 ml/s), the energy rate for the cascaded system shows a secondary rise to a peak value from around 60 to 90 mins. This is possibly due the phase change transition of erythritol (Fig. 3 (b)-4 ml/s) during this period which forces the outlet temperature to have an almost constant value thus increasing the thermal gradient between the top and the bottom of the storage tank since the inlet temperature of the storage tank continues to rise. The secondary peak value is barely evident in the single PCM system when charging with the lowest flow-rate.

For the higher charging flow-rate (8 ml/s), the cascaded storage system shows a slightly better performance between 20 and 70 mins. Once the phase change transition for erythritol at the bottom is complete, the energy rate values drop to lower values from 80 mins to the end of charging possibly due to the faster temperature rise at the bottom of the storage once erythritol has melted. It is important to note that the single PCM system shows a secondary peak value around 80 mins possibly due to the drop of thermal gradient of the outlet temperature between 60 and 80 mins (Fig. 3(a)-8 ml/s) for this system induced by possible external disturbances like heat losses.

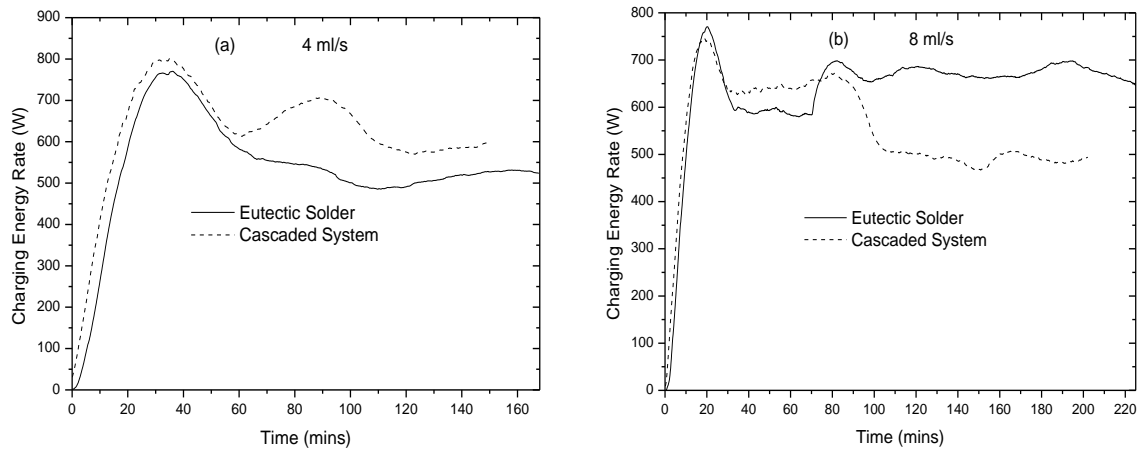


Figure 4. Charging energy rates for the two storage systems using low (4 ml/s) and high (8 ml/s) charging flow-rates.

Fig. 5 shows the charging exergy rates using low and high charging flow-rates. The exergy rate values are lower as compared to the energy rate values since heat losses are accounted for. For 4 ml/s, the cascaded storage system shows appreciably higher values after 60 mins, when erythritol at the bottom starts to melt. This melting process at the bottom for the cascaded system is depicted by the rise in the exergy rate values from 60 to 90 mins. For the single PCM system, the commencement of the melting process can also be qualitatively inferred from around 100 mins for the lowest flow-rate when the exergy rate profile starts to show a gradual slow rise until the end of charging.

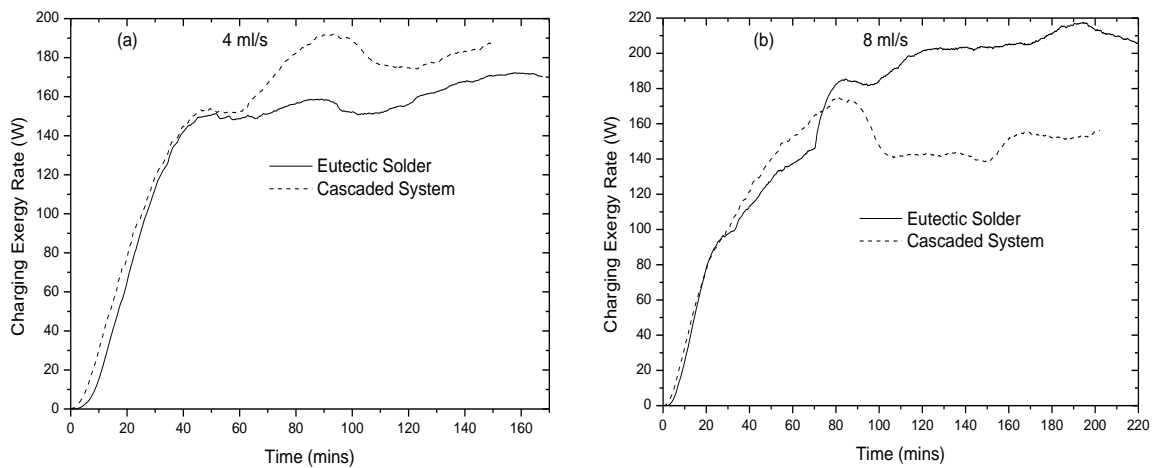


Figure 5. Charging exergy rates for the two storage systems using low (4 ml/s) and high (8 ml/s) charging flow-rate.

Increasing the flow-rate from 4 ml/s to 8 ml/s seems to show a faster rise of the exergy rate for the cascaded system to the peak value although lower exergy rate values are obtained. The charging exergy rates for the cascaded system are higher from around 30 mins to 70 mins when compared to the single PCM system. The drop in the exergy rate values after 70 mins for the cascaded system can also be used to infer the time when the phase change process at the bottom has finished, and the time when the temperatures at the bottom are increasing more rapidly after melting of erythritol due to the lower thermal mass at the bottom. The single PCM shows higher exergy rate values after 70 mins. The difference between the exergy rate values of the two storage

systems for the higher flow-rate is considerably higher as compared to the lower flow-rate after the PCM at the bottom of the cascaded storage system has melted. In general, it seems the storage advantages of the cascaded system in terms of the charging energy and exergy rates are more pronounced with the low flow-rate. Increasing the flow-rate tends to improve the storage performance of the single PCM in terms of these two evaluated quantities.

5. Conclusion

Two packed bed latent heat storage systems for medium temperatures were experimentally compared during charging cycles. The first storage system consisted of a packed bed of spherically encapsulated eutectic solder (Sn67Pb37). The second latent heat storage was a cascaded system consisting of 20 spherically encapsulated eutectic solder capsules at the top of the storage, and 20 spherically encapsulated erythritol capsules at the bottom in a storage ratio of 1:1. Sunflower Oil was used as the heat transfer fluid for the experiment tests. The cascaded latent heat showed greater values of the charging energy and exergy rate since two phase change transitions for the eutectic solder and erythritol release greater latent heat than the single PCM system during low flow-rate charging (4 ml/s). For charging with the higher flow-rate (8 ml/s), the cascaded storage system showed better energy and exergy charging rates before the bottom PCM melted. After melting of the lower temperature PCM at the bottom, the temperature increased at the bottom of the cascaded system, and the single PCM system showed higher charging energy and exergy rates. In general a cascaded system is cheaper as compared to a pure metallic PCM system, but its performance seemed to degrade when the lower temperature PCM melted during the charging cycles with the higher flow-rate.

6. Acknowledgement

The authors would like to thank the Material Science Innovation and Modelling (MASIM) research focus area of the North-West University for funding to carry out this research.

7. References

- [1] Kumaresan G, Vigneswaran VS, Esakkimuthu S, Velraj R. Performance assessment of a solar domestic cooking unit integrated with thermal energy storage system. *Journal of Energy Storage* 2016; 6: 70–79.
- [2] Shobo AB, Mawire A, Okello D. Experimental thermal stratification comparison of two storage systems. *Energy Procedia* 2017; 142: 3295–3300.
- [3] Mawire A, Performance of Sunflower Oil as a sensible heat storage medium for domestic applications. *Journal of Energy Storage* 2016; 5:1–9.
- [4] Wang Y, Wang L, Xie N, Lin X, Chen H. Experimental study on the melting and solidification behavior of erythritol in a vertical shell-and-tube latent heat thermal storage unit. *International Journal of Heat and Mass Transfer* 2016; 99:770–81.
- [5] Shobo AB, Mawire A. Experimental comparison of the thermal performances of acetanilide, meso-erythritol and an In-Sn alloy in similar spherical capsules. *Applied Thermal Engineering* 2017; 124:871–82.
- [6] Mawire A, Shobo AB. Investigation of In–48Sn as a phase change material candidate for thermal storage applications. *Renewable Energy and Environmental Sustainability* 2017; 2:20(1-5).
- [7] Peiró G, Gasia J, Miró M, Cabeza LF. Experimental evaluation at pilot plant scale of multiple PCMs (cascaded) vs. single PCM configuration for thermal energy storage. *Renewable Energy Engineering* 2015; 83:997–1011.
- [8] Yuan F, Li M, Ma Z, Jin B, Liu Z. Experimental study on thermal performance of high-temperature molten salt cascaded latent heat thermal energy storage system. *International Journal of Heat and Mass Transfer* 2018; 118:729–36.
- [9] Wu YK, Lin KL, Salam B. Specific heat capacities of Sn-Zn-Based solders measured using differential scanning calorimetry. *Journal of Electronic Materials* 2009; 38: 227–30.
- [10] Morando C, Fornaro O, Garbellini O, Palacio H. Thermal properties of Sn-based solder alloys. *Journal of Materials Science: Materials in Electronics* 2014; 25:3440–47.
- [11] Sn63Pb37 RA Solder Wire4880–4888 Technical Data Sheet 2018: <https://images-na.ssl-images-amazon.com/images/I/81h+ZhgF19L.pdf>, website accessed January 2018.
- [12] Mawire A, Lentswe KA, Shobo A. Performance comparison of four spherically encapsulated phase change materials for medium temperature domestic applications. *Journal of Energy Storage* 2019; 23: 469–79.

- [13] Lugolole R, Mawire A, Lentswe KA, Okello D, Nyeinga K. Thermal performance comparison of three sensible heat thermal energy storage systems during charging cycles. *Sustainable Energy Technologies and Assessments* 2018; 30: 37–51.